

Endocytosis of Murine Norovirus 1 into Murine Macrophages Is Dependent on Dynamin II and Cholesterol[∇]

Jeffrey W. Perry and Christiane E. Wobus*

Department of Microbiology and Immunology, University of Michigan Medical School, Ann Arbor, Michigan 48109-5620

Received 12 February 2010/Accepted 26 March 2010

Although noroviruses cause the vast majority of nonbacterial gastroenteritis in humans, little is known about their life cycle, including viral entry. Murine norovirus (MNV) is the only norovirus to date that efficiently infects cells in culture. To elucidate the productive route of infection for MNV-1 into murine macrophages, we used a neutral red (NR) infectious center assay and pharmacological inhibitors in combination with dominant-negative (DN) and small interfering RNA (siRNA) constructs to show that clathrin- and caveolin-mediated endocytosis did not play a role in entry. In addition, we showed that phagocytosis or macropinocytosis, flotillin-1, and GRAF1 are not required for the major route of MNV-1 uptake. However, MNV-1 genome release occurred within 1 h, and endocytosis was significantly inhibited by the cholesterol-sequestering drugs nystatin and methyl- β -cyclodextrin, the dynamin-specific inhibitor dynasore, and the dominant-negative dynamin II mutant K44A. Therefore, we conclude that the productive route of MNV-1 entry into murine macrophages is rapid and requires host cholesterol and dynamin II.

Murine noroviruses (MNV) are closely related to human noroviruses (HuNoV), the causative agent of most outbreaks of infectious nonbacterial gastroenteritis worldwide in people of all ages (4, 8, 19, 31, 43, 46, 83). Although a major public health concern, noroviruses have been an understudied group of viruses due to the lack of a tissue culture system and small animal model. Since the discovery of MNV-1 in 2003 (27), reverse genetics systems (10, 81), a cell culture model (84), and a small animal model (27) have provided the tools necessary for detailed study of noroviruses.

One largely unexplored aspect of norovirus biology is the early events during viral infection that are essential during viral pathogenesis. One of these early events is the attachment of the virus particle to the host. Attachment is mediated by the protruding domain of the MNV-1 capsid (29, 30, 73). For at least three strains (MNV-1, WU-11, and S99), the attachment receptor on the cell surface of murine macrophages is terminal sialic acids, including those found on the ganglioside GD1a (72). The use of carbohydrate receptors for cell attachment is shared with HuNoV, which utilize mostly histo-blood group antigens (HBGA) (18, 34, 70, 71). These carbohydrates are present in body fluids (saliva, breast milk, and intestinal contents) and on the surface of red blood cells and intestinal epithelial cells (33). Some HuNoV strains also bind to sialic acid or heparan sulfate (60, 69). However, despite evidence that for HuNoV HBGA are a genetic susceptibility marker (35), the presence of attachment receptors is not sufficient for a productive infection for either HuNoV (24) or MNV-1 (72). Although the cellular tropism of HuNoV is unknown, MNV infects murine macrophages and dendritic cells *in vitro* and *in*

vivo (80, 84). Following attachment, MNV-1 infection of murine macrophages and dendritic cells can proceed in the presence of the endosome acidification inhibitor chloroquine or bafilomycin A1, suggesting that MNV-1 entry occurs independently of endosomal pH (54). However, the cellular pathway(s) utilized by MNV-1 during entry remains unclear.

Viruses are obligate intracellular pathogens that hijack cellular processes to deliver their genome into cells. The most commonly used endocytic pathway during virus entry is clathrin-mediated endocytosis (41). Clathrin-coated vesicles form at the plasma membrane, pinch off by the action of the small GTPase dynamin II, and deliver their contents to early endosomes (12). For example, vesicular stomatitis virus (VSV) enters cells in this manner (66). However, viruses can also use several clathrin-independent pathways to enter cells, some of which require cholesterol-rich microdomains (i.e., lipid rafts) in the plasma membrane (56). The best studied of these is mediated by caveolin and was initially elucidated through studies of simian virus 40 (SV40) entry (1). SV40 uptake occurs via caveolin-containing vesicles that are released from the plasma membrane in a dynamin II-dependent manner and later fuse with pH-neutral caveosomes (28, 48, 53). Although caveolin-mediated endocytosis is a well-characterized form of cholesterol-dependent endocytosis, other entry mechanisms exist that are clathrin and caveolin independent (5, 14, 55, 57–59, 64, 78). In addition, macropinocytosis and/or phagocytosis can also play a role in viral entry (11, 13, 21, 36, 40, 42, 44, 45). However, the requirement for dynamin II in these processes is not fully understood.

Viral entry has been addressed primarily by pharmacologic inhibitor studies, immunofluorescence and electron microscopy, transfections of dominant-negative (DN) constructs, and more recently by small interfering RNA (siRNA) knockdown. Each of these approaches has some limitations; thus, a combination of approaches is needed to elucidate the mechanism of viral entry into host cells. For example, using electron and fluorescence microscopy, which require a high particle num-

* Corresponding author. Mailing address: Department of Microbiology and Immunology, 5622 Medical Sciences Bldg. II, 1150 West Medical Center Dr., University of Michigan Medical School, Ann Arbor, MI 48109-5620. Phone: (734) 647-9599. Fax: (734) 764-3562. E-mail: cwobus@umich.edu.

[∇] Published ahead of print on 7 April 2010.

ber, does not allow the differentiation of infectious and non-infectious particles. Alternatively, the use of pharmacological inhibitors can result in off-target effects, including cytotoxicity. A recent approach used the photoreactive dye neutral red (NR) in an infectious focus assay to determine the mechanism of poliovirus entry (6). Cells were infected in the dark in the presence of neutral red, and virus particles passively incorporated the dye. Upon exposure to light, the neutral red dye cross-linked the viral genome to the viral capsid, thus inactivating the virus. Infectious foci were counted several days later. This assay was performed in the presence of various pharmacologic inhibitors of endocytosis. When an inhibitor blocked a productive route of infection, the number of infectious foci was significantly less than that for an untreated control. Major advantages of this technique over traditional assays are the ability to treat cells with pharmacologic inhibitors only during the viral entry process, the reduction of cytotoxicity, and the ability to infect with a low multiplicity of infection (MOI). Furthermore, infectious virus that is prohibited from uncoating is inactivated by illumination. Therefore, only virus particles leading to a productive infection in the presence or absence of the various inhibitors are measured. We successfully adapted this assay for use with MNV-1. Together with the use of pharmacological inhibitors, DN constructs, and siRNA knockdown, we demonstrate that the major MNV-1 entry pathway into murine macrophages resulting in a productive infection occurred by endocytosis and not phagocytosis or macropinocytosis in a manner that was clathrin and caveolin 1, flotillin 1, and GRAF1 independent but required dynamin II and cholesterol.

MATERIALS AND METHODS

Cell culture and mice. RAW 264.7 cells were purchased from ATCC (Manassas, VA) and maintained as previously described (84). Swiss Webster mice were purchased from Charles River. Caveolin-1 knockout mice (number 004585) and matched control mice (B6129SF2/J, number 101045) were purchased from Jackson Laboratories. Bone marrow-derived macrophages (BMDMs) were isolated as previously described (84).

Virus stocks. The plaque-purified MNV-1 clone (GV/MNV1/2002/USA) MNV-1.CW3 was used at passage 6 for all experiments (74). To generate NR-containing viral stocks, all activities were carried out in the dark. RAW 264.7 cells were infected with MNV-1 at an MOI of 0.05 and incubated for 40 h in the presence of 10 μ g/ml neutral red (Sigma-Aldrich, MO; N2880). Cells were freeze-thawed twice to release virus, and single-use aliquots were stored at -80°C . All NR virus preparations exhibited a minimum two-log reduction in viral titers upon light exposure as determined by plaque assay compared to a control virus not exposed to light. Vesicular stomatitis virus (Indiana strain) was propagated in Vero cells, and single-use aliquots were stored at -80°C .

Growth curves (dynasore inhibition). RAW 264.7 cells or BMDMs were plated at 2×10^5 cells/ml in 12-well plates and allowed to attach overnight. Cells were then incubated with the indicated concentrations of dynasore (Sigma-Aldrich, MO) in dimethyl sulfoxide (DMSO) or vehicle control for 30 min. Cells were infected with MNV-1 or VSV at the indicated MOI in the presence of dynasore or vehicle control for 60 min on ice. The cells were washed and fresh media containing inhibitor added. Infection was allowed to proceed until the indicated time point, when the cells were freeze-thawed twice, and viral titers were determined by plaque assay as previously described (84).

Immunofluorescence assay. RAW 264.7 cells or BMDMs were plated at 2×10^5 cells/ml in 6-well plates containing sterile glass coverslips (Fisher Scientific) and allowed to attach overnight. Cells were then incubated with the indicated concentrations of methyl- β -cyclodextrin (M β CD) (Sigma-Aldrich, MO), fetal bovine serum (FBS) and M β CD, or vehicle control (DMSO) for 60 min. Cells were infected with MNV-1 or VSV at the indicated MOI in the presence of inhibitor or vehicle control for 60 min on ice. Cells were washed and fresh media containing inhibitor added. Infection proceeded until the indicated time point when the cells were fixed with 4% paraformaldehyde in phosphate-buffered saline (PBS) for 10 min, washed once with PBS, and stained for the viral

nonstructural protein VPg (81) or VSV matrix (38) as previously described (54). Briefly, cells were incubated with a monoclonal mouse antibody raised against MNV-1 VPg (81) diluted 1:5,000 or VSV matrix (38) diluted 1:10,000 in wash buffer (PBS, 1% bovine serum, 1% goat serum, 0.1% Triton X-100) for 1 h. Cells were then washed three times with wash buffer before incubation with an Alexa 594-conjugated goat anti-mouse antibody diluted 1:5,000 (Invitrogen, CA) for 1 h. Cells were washed three times as described above and mounted using Prolong Gold Antifade with DAPI (4', 6-diaminidino-2-phenylindole) (Invitrogen, CA). A total of 500 DAPI-stained cells were examined using the Olympus IX70 inverted microscope at the Center for Live Cell Imaging at the University of Michigan. Cells that had an average fluorescence intensity of at least three times the average background fluorescence intensity as determined by the MetaMorph Premier version 6.3 image analysis software (Molecular Devices, Downingtown, PA) were counted as infected cells. The number of infected cells was then normalized to the no-treatment control.

NR assay. RAW 264.7 cells were plated at 1×10^6 cells/ml in 6-well plates and allowed to attach overnight. For pretreatments, cells were incubated with the indicated concentrations of chloroquine, neuraminidase, dynasore, chlorpromazine, sucrose, nystatin, cytochalasin D, amiloride (EIPA [5-ethyl-N-isopropyl amiloride]) (all purchased from Sigma-Aldrich, MO), or vehicle control for 30 min, or 60 min for M β CD. Cells were infected with MNV-1 at an MOI of 0.001 in the presence of inhibitor or vehicle control. After 60 min, the cells were illuminated, and a plaque assay was performed by adding an agarose overlay and staining cells with neutral red after 48 to 72 h. In the case of chlorpromazine and sucrose treatments, cells were infected only for 30 min to maintain cell viability. To assess the nonspecific effects of drugs on later stages of the viral life cycle (posttreatment), cells were infected for 60 min at an MOI of 0.001 in the absence of inhibitors, the infection was stopped by illumination, and inhibitors were added back at the same concentration and length of time as the pretreatments. To determine the dynamic range of the experiment, untreated cells were infected at an MOI of 0.001 and illuminated immediately after addition of virus (0 min) or 60 min after addition of virus.

WST-1 cell viability assay. RAW 264.7 cells and BMDMs were plated at 2×10^5 cells/ml in a 96-well plate. Cells were pretreated with chloroquine, neuraminidase, dynasore, chlorpromazine, sucrose, nystatin, cytochalasin D, amiloride (EIPA) (all purchased from Sigma-Aldrich, MO), or vehicle control for 30 min, or 60 min for M β CD. Cells were then treated in the presence of inhibitor or vehicle control for the length of time indicated (Table 1). M β CD combination treatments were performed by 1-h treatment of M β CD followed by 60-min treatment of the other drug in media lacking FBS. At that time, media were removed, and media containing 10% WST-1 reagent (Roche) were added to cells. Cell viability was determined following the manufacturer's recommendations at 120 min after addition of reagent.

Transfection of RAW 264.7 cells. Cells were plated at a density of 4.0×10^5 cells/ml in 6-well plates and allowed to attach overnight. The following day, cells were transfected using Lipofectamine 2000 (Invitrogen) following the manufacturer's protocol. Briefly, media were replaced with Optimum media (Invitrogen), and a transfection solution containing 5 μ g of plasmid DNA and 8 μ l of Lipofectamine 2000 (Invitrogen) was prepared. Cells were incubated with the transfection reagent for 8 h and washed with media. Cells were infected 48 h after transfection with MNV-1 as described above. At 12 h postinfection (hpi), infected cells were processed for immunofluorescence analysis as described above. However, instead of quantitating 500 DAPI-stained cells, 500 DAPI-stained and green fluorescent protein (GFP)-expressing cells with an average fluorescence intensity at least three times the background's average fluorescence intensity were quantitated as infected cells. The dynamin II wild-type (wt) and DN (K44A) constructs, both containing proteins fused to GFP, were kindly provided by Mark McNiven (Mayo Institute, Rochester, MN) (7). The EPS 15 wt and DN (Δ 95/295) constructs, both containing proteins fused to GFP, were kindly provided by A. Benmerah (INSERM, Paris, France) (3). The RAC 1 wt and DN (T17N) constructs, both containing proteins fused to GFP, as well as the GFP-only construct, were kindly provided by J. Swanson (University of Michigan, Ann Arbor, MI) (26a). The caveolin 1 DN construct (GFP fused to the C terminus of wt Cav1) was provided by B. Tsai (University of Michigan, Ann Arbor, MI) (53).

siRNA knockdown. RAW 264.7 cells were plated at a density of 2×10^5 cells/ml in a 6-well plate and allowed to attach overnight. The next day, cells were washed once with Accell siRNA delivery media (Dharmacon) before incubation with Accell siRNA delivery media containing 1 μ M the indicated Accell siRNA. The cells were incubated for 72 h, washed once with DMEM media, and infected as described above. At 12 h postinfection, virus-infected cells were analyzed by an immunofluorescence assay as described above. Cells treated in parallel were analyzed by SDS-PAGE and then by Western blot analysis to ensure effective knockdown of protein levels. The following sequences were used: clathrin heavy

TABLE 1. Inhibitor treatments do not significantly affect viability of RAW 264.7 cells and BMDMs^a

Inhibitor	Cell viability (%) (SD)		
	1 h	8 h	12 h
RAW 264.7 cells			
No-treatment control	100 (±18)	100 (±16)	100 (±14)
40 μM chlorpromazine	99 (±10)	ND	ND
200 μM chloroquine	125 (±9)	ND	ND
20 μM cytochalasin D	91.9 (±8)	ND	ND
40 μM dynasore	ND	125 (±39)	ND
80 μM dynasore	117 (±25)	116 (±30)	ND
200 μM EIPA	80.3 (±8)	ND	ND
2 mM MβCD	120 (±16)	ND	122 (±24)
2 mM MβCD + FBS	88 (±14)	ND	102 (±22)
2.5 mU neuraminidase	123 (±6)	ND	ND
50 μM nystatin	125 (±18)	ND	ND
300 μM Sucrose	101 (±16)	ND	ND
2 mM MβCD + 40 μM chlorpromazine	58 (±3)	ND	ND
2 mM MβCD + 20 μM cytochalasin D	92 (±13)	ND	ND
2 mM MβCD + 80 μM dynasore	93 (±8)	ND	ND
2 mM MβCD + 200 μM EIPA	97 (±14)	ND	ND
Primary bone marrow-derived macrophages			
No-treatment control	ND	ND	100 (±10)
80 μM dynasore	ND	ND	76.3 (±7)
160 μM dynasore	ND	ND	79.3 (±12)
2 mM MβCD	ND	ND	96 (±7)
2 mM MβCD + FBS	ND	ND	113 (±8)

^a RAW 264.7 cells and BMDMs were pretreated with inhibitors as described in the text. After the treatment period, cells were washed once with medium, and medium containing 10% WST-1 (Roche) was added to the cells. After 120 min of incubation at 37°C and 5% CO₂, optical densities at 420 nm were read on a spectrophotometer. Cell viability was normalized to that of vehicle control-treated cells set at 100%. ND, not determined.

chain (CHC) (GUGUUAUGGAGUAUAUAAA), caveolin 1 (CAV-1) (CCAUAUCUCAUAUAUAUC), flotillin-1 (CUAUUUAACUCCUGAUUA), and GRAF1 (UUAUCUCCCAUCAGCACAGAUUAUC).

Western blot analysis. Whole-cell lysates from siRNA-transfected RAW 264.7 cells were generated by adding 2× SDS-PAGE sample buffer to cells. Samples were boiled for 5 min and separated by SDS-PAGE. Proteins were then transferred to nitrocellulose (Bio-Rad). Membranes were blocked in 5% nonfat dry milk and incubated with primary antibodies and then with horseradish peroxidase in 5% nonfat dry milk. The following antibodies were used: clathrin heavy chain (no. 610500; BD Transduction Laboratories), caveolin 1 (no. 610406; BD Transduction Laboratories), flotillin-1 (no. sc-25506; Santa Cruz Biotech), and GRAF1 (kindly provided by R. Lundmark, Umea University, Sweden) (37). Band densities were determined using Adobe Photoshop (CA). Briefly, a selection box was created around the band of interest, and the mean pixel intensity determined. The same selection box was used for other bands, and also a region without a signal was used as a background control. The mean pixel intensity of the background control was subtracted from all other mean pixel intensities. The background-subtracted mean pixel intensities were normalized to the value for the nontargeting (NT) siRNA sample, which was set to 100%.

Fluorescent transferrin and cholera toxin subunit B internalization assay. RAW 264.7 cells or BMDMs were plated at 2×10^5 cells/ml in 6-well plates containing sterile glass coverslips (Fisher Scientific) and allowed to attach overnight. Cells were pretreated with increasing concentrations of chlorpromazine, sucrose, nystatin, or vehicle control for 30 min, or 60 min for MβCD. Cells were then incubated in 10 μg/ml fluorescently labeled cholera toxin subunit B (Invitrogen) or 50 μg/ml transferrin (Invitrogen, CA) in the presence of inhibitor. Cells were washed, and media containing inhibitor or vehicle control were added back for 5 min for transferrin or 60 min for cholera toxin subunit B. Cells were fixed in 4% paraformaldehyde and mounted with Prolong Gold Antifade with DAPI (Invitrogen, CA). Cells were examined using the Olympus IX70 inverted microscope at the Center for Live Cell Imaging at the University of Michigan, and images were acquired using the Metamorph Premier version 6.3 image analysis software (Molecular Devices, Downingtown, PA).

Listeria monocytogenes infection of RAW 264.7 cells. RAW 264.7 cells were plated at 2×10^5 cells/ml in 6-well plates containing sterile glass coverslips (Fisher Scientific) and allowed to attach overnight. Cells were pretreated with increasing concentrations of cytochalasin D, amiloride (EIPA), or vehicle control. *Listeria monocytogenes* strain 10403S (a kind gift from M. O'Riordan, University of Michigan, Ann Arbor, MI) was grown overnight to an optical density at 600 nm (OD₆₀₀) of 1.2 in brain heart infusion (BHI; Sigma Aldrich). Bacteria were pelleted and resuspended in PBS. Cells were infected at an MOI of 1 for 30 min at 37°C. Cells were washed with PBS and 50 μg/ml gentamicin (Fisher Scientific) added to inhibit replication of noninternalized bacteria. After 1 h postinfection, cells were lysed in sterile water and plated onto LB plates. CFU were quantitated 24 h after incubation at 37°C and normalized to the vehicle control.

Statistics. Error bars in the figures represent the standard error between independent experiments. Statistical analysis was performed using Prism software version 5.01 (GraphPad Software, CA). The two-tailed Student *t* test was used to determine statistical significance.

RESULTS

Development of a neutral red infectious center assay to study MNV-1 entry. Viral entry is studied by a combination of different methods, one of which is the inhibition of proteins critical for specific endocytic pathways with pharmacologic inhibitors. However, these inhibitors often have off-target effects, including cytotoxicity for the cell type analyzed. To address this, we empirically determined minimal effective concentrations for RAW 264.7 cells or BMDMs that inhibited uptake of fluorescently labeled transferrin and cholera toxin subunit B (Fig. 1) and measured cell viability (Table 1) at these concentrations by WST-1 (Roche), which measures mitochondrial dehydrogenase activity, for all inhibitors used. Cell viability was mostly unaffected at the concentrations used and typically remained above 80% of that of untreated controls. A significant reduction in the signal intensity of fluorescently labeled transferrin was observed for both chlorpromazine- and sucrose-treated cells but not after MβCD treatment compared to untreated cells (Fig. 1A to E), indicating a block in transferrin uptake. Although the intensity of the fluorescently labeled cholera toxin subunit B signal did not significantly change, the localization of the signal shifted from a mainly punctate cytoplasmic signal to a predominantly plasma membrane location after treatment of cells with MβCD or nystatin compared to untreated cells or cells treated with MβCD with FBS that had reconstituted cholesterol levels (Fig. 1F to I). This suggests that cholera toxin subunit B was no longer efficiently internalized in the presence of these concentrations of MβCD and nystatin.

In addition, we adapted an assay to study the productive entry of MNV-1 using abbreviated treatments of pharmacological inhibitors as another way to limit off-target effects, including cytotoxicity. We modified the neutral red infectious center assay published for poliovirus, which quantitatively determines the number of viral entry events leading to a productive infection (6). MNV-1 stocks were generated in the presence of the vital dye neutral red. The neutral red dye passively incorporates into the virus particle. Upon illumination, the dye activates and cross-links proteins and nucleic acids. Since the dye and viral genome are trapped in the virion, viral genome that has not been uncoated will be cross-linked irreversibly to the protein capsid, thus inactivating the virus particle. However, the process of viral uncoating allows the neutral red and viral genome to disassociate and thereby become light insen-

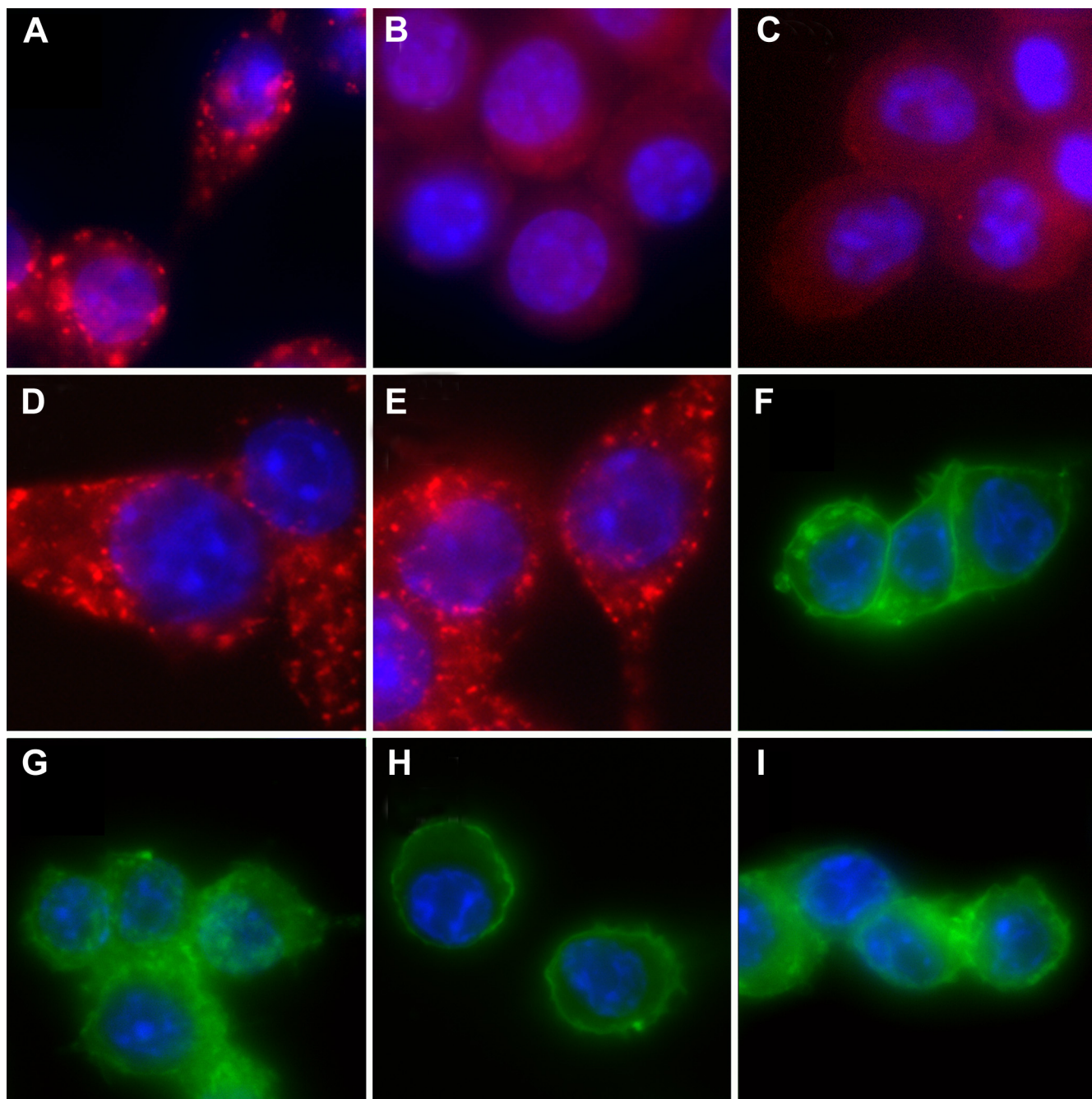


FIG. 1. Uptake of fluorescently labeled transferrin is inhibited by a hypotonic solution of sucrose or chlorpromazine. RAW 264.7 cells were incubated with vehicle control (A, D, and G), chlorpromazine (B), a hypotonic solution of sucrose (C), or nystatin (F) for 30 min or M β CD (E and H) or M β CD and 10% FBS (I) for 60 min before incubation with 50 μ g/ml fluorescently labeled transferrin (A to E) or 10 μ g/ml fluorescently labeled cholera toxin subunit B (F to I). Cells were washed and media containing inhibitor or vehicle control added back for 5 min for transferrin or 60 min for cholera toxin subunit B. Cells were fixed in 4% paraformaldehyde and mounted with Prolong Gold Antifade with DAPI (Invitrogen, CA). Cells were examined using an Olympus IX70 inverted microscope and images acquired using the Metamorph Premier version 6.3 image analysis software (Molecular Devices, Downingtown, PA).

sitive. Using MNV-1 particles containing neutral red, we infected RAW 264.7 cells at room temperature for 0, 15, 30, 45, 60, or 75 min before exposure to light for 10 min to determine the entry kinetics for MNV-1 (Fig. 2A). This revealed that approximately 100% of NR-containing MNV-1 becomes light insensitive 60 min after addition to RAW 264.7 cells (Fig. 2B).

This indicated that the kinetics of RNA release (i.e., uncoating) as measured by this assay had a half-life ($t_{1/2}$) of 33 ± 2 min. This is similar to data from poliovirus genome release in HeLa cells ($t_{1/2} = 22 \pm 3$ min) (6).

To verify the applicability of the NR assay for studying MNV-1 entry, we determined the effect of two known inhibi-

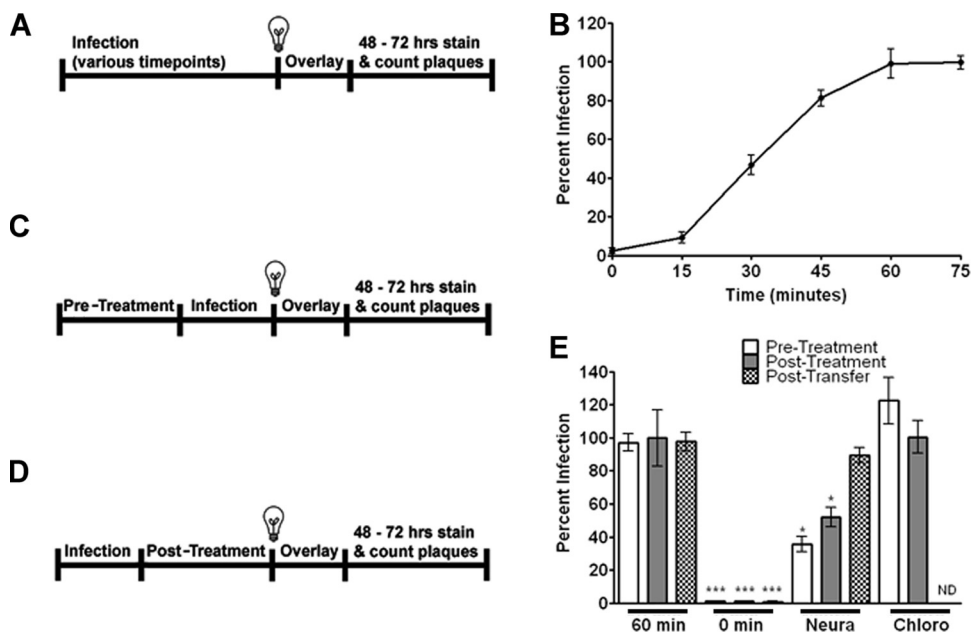


FIG. 2. Neutral red (NR) infectious center assay confirms a pH-independent and sialic acid-dependent entry mechanism for MNV-1. (A, C, and D) Flow charts of the NR assay describing different treatment conditions. (A and B) MNV-1 rapidly becomes insensitive to light exposure. RAW 264.7 cells were infected with NR-containing virus at an MOI of 0.001, rocked at room temperature, exposed to light at 0, 15, 30, 45, 60, and 75 min postinfection (pi), and overlaid with agarose, and plaques were counted 48 to 72 h pi. (C, D, and E) MNV-1 entry is sialic acid dependent and pH independent. (C and E, pretreatment) RAW 264.7 cells were pretreated with 2.5 mU/ml *Vibrio cholerae* neuraminidase (Neura) or 200 μ M chloroquine (Chloro) for 30 min, infected by rocking for 60 min, and overlaid with media containing agarose, and plaques were counted 48 to 72 h pi. (D and E, posttreatment) Alternatively, RAW 264.7 cells were infected with an MOI of 0.001 for 60 min and then posttreated with 2.5 mU/ml *Vibrio cholerae* neuraminidase (Neura) or 200 μ M chloroquine (Chloro) for a total of 90 min before performing the NR assay. (E, posttransfer) In case of *Vibrio cholerae* neuraminidase treatment, RAW 264.7 cells were posttreated as described, scraped, and transferred to an untreated monolayer before a plaque assay was performed and viral titers were determined. *, $P < 0.05$.

tors: chloroquine, an endosomal acidification inhibitor, and *Vibrio cholerae* neuraminidase, an enzyme that hydrolyzes terminal sialic acids on the host cell surface (54, 72). These inhibitors have either no effect on MNV-1 entry (chloroquine) (54) or significantly decrease MNV-1 infection in murine macrophages (*Vibrio cholerae* neuraminidase) (72). RAW 264.7 cells were pretreated with 200 μ M chloroquine or 2.5 mU/ml *Vibrio cholerae* neuraminidase for 30 min prior to infection with NR-containing MNV-1 in the dark for 60 min at an MOI of 0.001. RAW 264.7 cells were then exposed to light for 10 min, washed, and incubated for 48 to 72 h with an agarose media overlay, and virus plaques were quantitated (Fig. 2C). To ensure that the inhibitors did not exhibit off-target effects on stages of the viral life cycle other than entry, a posttreatment (Fig. 2D) was performed for each inhibitor. These treatments were performed for each inhibitor assayed and equaled the length of the pretreatment. Consistent with our published results (54, 72), MNV-1 entry as measured by the NR assay was not inhibited by pretreatment of cells with 200 μ M chloroquine but was inhibited by pretreatment with *Vibrio cholerae* neuraminidase, validating the NR assay (Fig. 2E). Posttreatment of cells with 200 μ M chloroquine did not inhibit MNV-1 infection, confirming it has no effect on other stages of the viral life cycle (Fig. 2E). However, posttreatment of *Vibrio cholerae* neuraminidase led to a significant decrease in viral infection (Fig. 2E). We reasoned that this was due to the dependence of viral infection and spread on sialic acid (i.e., development of plaques). Therefore, we transferred cells to an untreated

monolayer of RAW 264.7 cells to circumvent this potential problem. RAW 264.7 cells were infected for 60 min with MNV-1 and illuminated to inactivate virus. Cells were then treated with *Vibrio cholerae* neuraminidase for 90 min, washed, scraped from the plate, and added to an untreated monolayer of RAW 264.7 cells (posttransfer). No significant reduction in MNV-1 infection was observed (Fig. 2E). This demonstrated that MNV-1 entry but not later steps of the viral life cycle were inhibited by *Vibrio cholerae* neuraminidase. Taken together, these results confirm studies from our laboratory (54, 72) that MNV-1 enters RAW 264.7 cells in a sialic acid-dependent but pH-independent manner and validate the use of the NR assay for studying the infectious entry pathway of MNV-1.

MNV-1 entry into murine macrophages requires dynamin II

Dynamin II is a small GTPase that functions by pinching off endosomes from the cell's plasma membrane (68). Its function is required for clathrin-, caveolin-, and cholesterol-dependent endocytosis pathways but not clathrin- and caveolin-independent processes (17, 41). The activity of dynamin II in phagocytosis has been suggested, but various mechanisms of viral entry through phagocytosis do not require it (12). To determine the role of dynamin II during MNV-1 infection, we obtained the small molecule inhibitor dynasore, which specifically inhibits dynamin I, dynamin II, and Drp 1 (39). Dynamin I is activated only in neuronal cells, and Drp 1 is confined to the mitochondria (49, 67). Therefore, we reason that dynasore affects dynamin II in murine macrophages. RAW 264.7 cells were pretreated and infected at an MOI of 5 with MNV-1 or

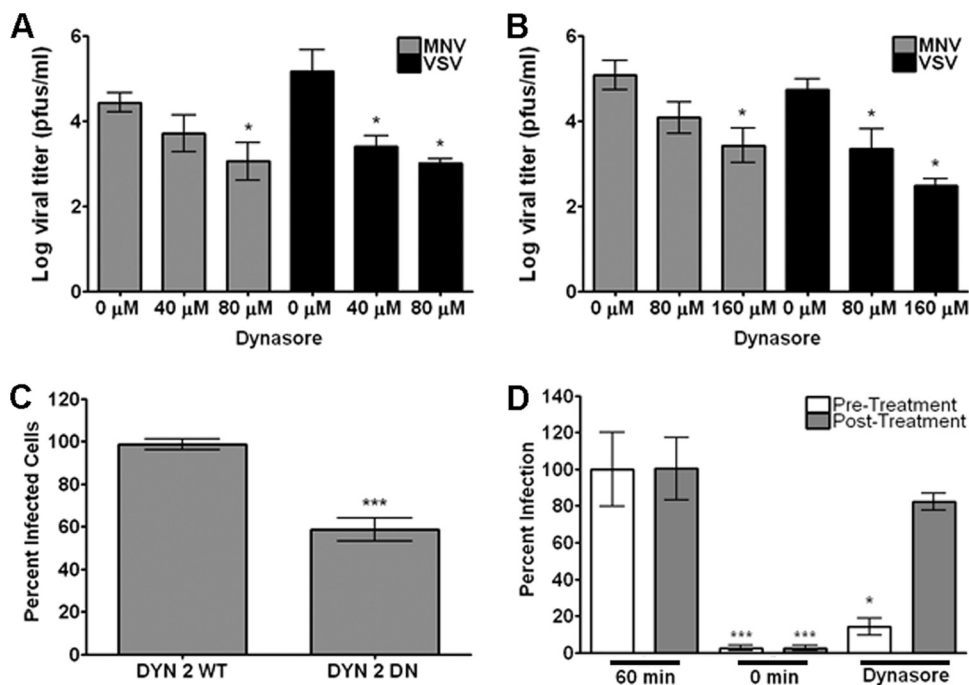


FIG. 3. MNV-1 infection requires dynamin II. RAW 264.7 cells (A) and BMDMs (B) were pretreated with dynasore at the indicated concentration for 30 min, infected with MNV-1 or VSV on ice for 1 h, and washed with PBS. At 8 h (RAW 264.7 cells) or 10 h (BMDMs) postinfection, cells were freeze-thawed two times and viral titers determined by plaque assay. (C) RAW 264.7 cells were transfected with a wt and DN construct of GFP-tagged dynamin II and then infected with MNV-1 (MOI of 10) for 12 h. The number of VPg-expressing cells was determined by immunofluorescence and normalized to the wt control. (D) RAW 264.7 cells were either pretreated (pretreatment) or treated for 60 min postinfection (posttreatment) with 80 μ M dynasore before performing a plaque assay and determining viral titers. *, $P < 0.05$; ***, $P < 0.001$.

VSV in the presence of increasing amounts of dynasore or DMSO, and viral titers were determined 8 h postinfection (Fig. 3A). MNV-1 viral titers were significantly inhibited by dynasore pretreatment in a dose-dependent manner with an approximately 1.5-log inhibition in viral titers at 80 μ M dynasore (Fig. 3A). VSV, a virus that requires dynamin II for its uptake via clathrin-mediated endocytosis (66), was used as a positive control and showed a significant decrease in viral titers at both concentrations of dynasore. Similar results were observed when BMDMs were infected, although higher effective concentrations of dynasore were needed in primary cells (Fig. 3B). Cell viability of treated cultured and primary macrophages was not significantly affected at these concentrations of inhibitor (Table 1). These results demonstrated that dynamin II plays a role in MNV-1 infection.

To further validate these results and look at earlier stages in the viral life cycle, the effect of the dynamin II DN construct K44A (7) on MNV-1 nonstructural gene expression was tested. Due to the poor transfection efficiency of primary macrophages, these experiments were performed only with RAW 264.7 cells. Cells were transfected with GFP-tagged wt and DN constructs. After 48 h, RAW 264.7 cells were infected with MNV-1 and VPg expression was measured by immunofluorescence assay as previously described (54). The number of cells expressing VPg was quantitated and normalized to GFP-tagged wt dynamin II-expressing cells. A significant decrease in cells expressing VPg was observed with the DN construct com-

pared to the wt control (Fig. 3C). These results demonstrated that MNV-1 gene expression requires dynamin II.

To determine the role of dynamin II during MNV-1 entry, we tested the effect of dynasore in the NR assay (Fig. 3D). Cell viability of treated cells was unaffected at these concentrations (Table 1). RAW 264.7 cells were pretreated with dynasore or vehicle control for 30 min and infected with NR-containing MNV-1, and the NR assay was performed as described above. A significant decrease in the number of plaques was observed for the pretreatment but not posttreatment samples, indicating MNV-1 entry required dynamin II. Together, these results demonstrated that dynamin II plays a role during MNV-1 entry into murine macrophages. However, the inability to completely block viral entry suggested a dynamin II-independent form(s) of endocytosis may also play a role during MNV-1 entry.

MNV-1 entry into murine macrophages is clathrin independent. Clathrin-mediated endocytosis requires dynamin II (16). In addition, feline calicivirus (FCV), a member of the calicivirus family, like MNV-1, has been shown to enter cells through this process (65). Therefore, we determined the role of clathrin during MNV-1 entry. To test this, we first used two pharmacologic inhibitors of clathrin-mediated endocytosis, chlorpromazine and a hypotonic solution of sucrose, in the NR assay. Chlorpromazine is an inhibitor of clathrin lattice polymerization (79), while a hypotonic solution of sucrose inhibits clathrin-coated pit formation in the plasma membrane (26). However, both inhibitors have known off-target effects (26, 63).

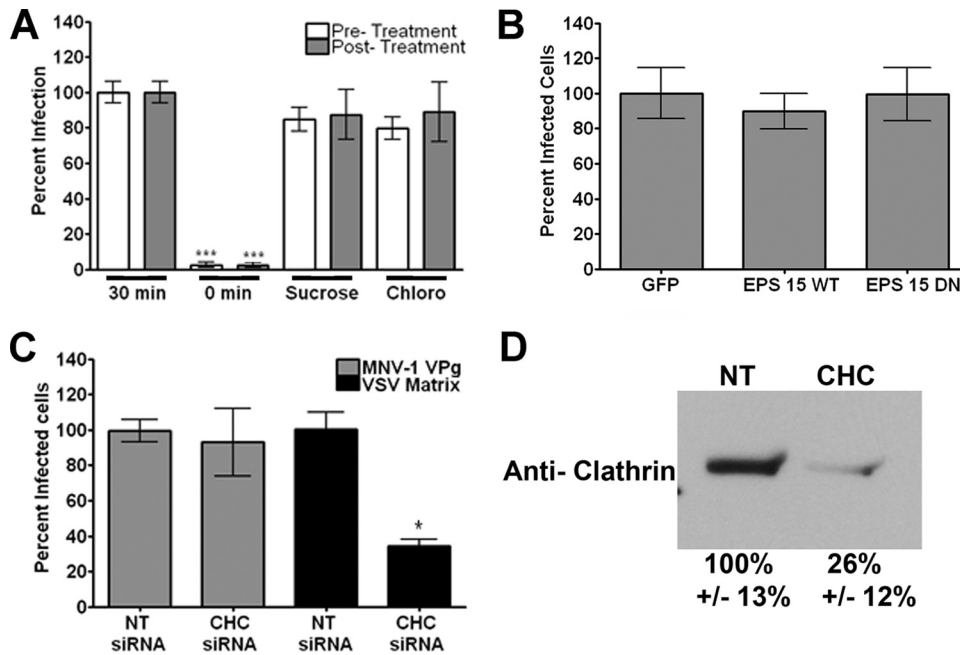


FIG. 4. MNV-1 infection is clathrin independent. (A) RAW 264.7 cells were infected with NR-containing virus at an MOI of 0.001 and rocked at room temperature for 60 min. RAW 264.7 cells were either pretreated (pretreatment) or treated for 60 min pi (posttreatment) with 40 μ M chlorpromazine (Chloro) or 300 mM sucrose. (B) RAW 264.7 cells were transfected with a GFP-only (GFP), GFP-tagged wt (EPS 15 wt), or DN construct (EPS 15 DN) of EPS 15 and then infected with MNV-1 at an MOI of 10 for 12 h. The number of VPg-expressing cells was determined by immunofluorescence and normalized to the value for the GFP-only control. (C) RAW 264.7 cells were incubated with an Accell siRNA clathrin heavy-chain construct (CHC siRNA) or a nontargeting construct (NT siRNA) (Dharmacon) for 72 h. Cells were then infected with MNV-1 or VSV at an MOI of 10. The number of VPg-expressing cells was determined by immunofluorescence 12 h after infection and normalized to the value for the NT control. (D) To verify clathrin heavy-chain protein knockdown, protein samples from cells expressing each siRNA construct were analyzed by immunoblotting for clathrin heavy chain, and protein levels were quantitated as described in the text. *, $P < 0.05$; ***, $P < 0.001$.

Furthermore, these inhibitors are relatively cytotoxic to RAW 264.7 cells. To maintain cell viability above 80% and minimize side effects, RAW 264.7 cells were pretreated for 30 min with 40 μ g/ml chlorpromazine or 300 mM sucrose, and the infection (performed in the presence of inhibitor) was reduced to 30 min. At these concentrations, we observed a significant decrease in the uptake of fluorescently labeled transferrin, a known clathrin-mediated endocytosis cargo protein (15), but not of fluorescently labeled cholera toxin B subunit (Fig. 1B and C and data not shown). We saw no significant reduction in MNV-1 entry with either chlorpromazine or sucrose treatment (Fig. 4A). Furthermore, posttreatment with these inhibitors did not affect MNV-1 infection (Fig. 4A). These results suggested MNV-1 entry is clathrin independent.

To confirm this finding, we tested wt and DN constructs of EPS 15, a required adaptor protein for clathrin-mediated endocytosis, for their effect on MNV-1 gene expression (Fig. 4B). EPS 15 directly links cargo proteins with the clathrin-coated pit adaptor protein 2 (AP-2) (3). Overexpression of the DN construct of EPS 15 selectively inhibits this process. RAW 264.7 were transfected with plasmids expressing GFP alone, GFP-tagged wt EPS 15, or GFP-tagged DN EPS 15 prior to infection, and virus-infected cells were quantitated by staining for VPg (Fig. 4B). We observed no significant change in the number of VPg-expressing cells in DN EPS 15 compared to those of wt-transfected or GFP-alone controls. These results further support the idea that clathrin played no role during MNV-1 infection.

However, not all clathrin-mediated endocytosis cargo requires EPS 15 (62). Therefore, we tested the role of clathrin during MNV-1 infection by siRNA knockdown of clathrin heavy chain (CHC). We obtained siRNA transfection efficiencies of over 93% for RAW 264.7 cells as determined by fluorescence-activated cell sorter analysis using a fluorescently labeled Accell siRNA construct from Dharmacon (data not shown). RAW 264.7 cells were transfected with an Accell siRNA for the CHC or an NT siRNA and infected with MNV-1 or VSV for 12 h at an MOI of 10. Infected cells were quantified by immunofluorescence as described above and stained for MNV-1 VPg or the VSV matrix protein (Fig. 4C). No significant decrease of VPg-expressing cells was observed with CHC- compared to NT-transfected cells after MNV-1 infection (Fig. 4C). In contrast, a significant decrease of matrix-expressing cells was observed in CHC- compared to NT-transfected cells after VSV infection (Fig. 4C). This is consistent with a previous study in which CHC knockdown significantly reduced VSV infection (66). In addition, depletion of CHC was confirmed by analyzing protein levels of CHC by immunoblotting (Fig. 4D). CHC protein levels in CHC siRNA-expressing cells were reduced to 26% \pm 12% of wt levels in NT siRNA-expressing cells. Taken together, these data demonstrated that clathrin plays no role in MNV-1 entry or infection.

MNV-1 entry into murine macrophages is caveolin 1 independent. Another pathway dependent on dynamin II is caveolin-mediated endocytosis (25, 50). Caveolin 1-associated vesic-

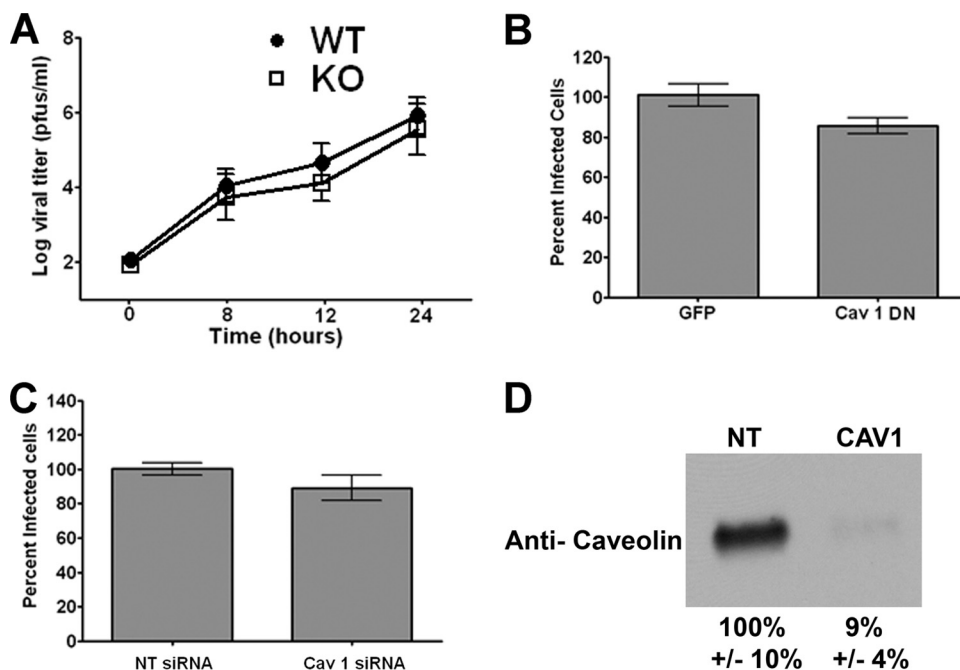


FIG. 5. MNV-1 infection is caveolin independent. (A) BMDMs were isolated from caveolin 1 knockout mice and wt controls and infected with MNV-1 at an MOI of 2. Viral titers were determined at times indicated. (B) RAW 264.7 cells were transfected with a DN GFP-tagged caveolin 1 (CAV 1 DN) and a GFP-only control (GFP) construct and infected with MNV-1 at an MOI of 10 for 12 h. VPg-expressing cells were determined by immunofluorescence and normalized to the value for the GFP-only control. (C) RAW 264.7 cells were incubated with an Accell siRNA caveolin 1 construct (CAV 1 siRNA) or a nontargeting construct (NT siRNA) (Dharmacon) for 72 h. Cells were then infected with MNV-1 or VSV at an MOI of 10, and VPg expression was determined by immunofluorescence 12 h after infection. The number of VPg-expressing cells was normalized to the value for the NT control. (D) To verify caveolin 1 protein knockdown, protein samples from cells expressing each siRNA construct were analyzed by immunoblotting for caveolin 1 and quantitated as described in the text.

cles can traffic to acidic early endosomes (52) or neutral pH caveosomes (53). Furthermore, previous data from our laboratory have shown that MNV-1 infection of murine macrophages and dendritic cells is not inhibited by the endosome acidification inhibitor bafilomycin A or chloroquine (54). Trafficking of MNV-1 to a pH-neutral compartment, such as the caveosome, would be consistent with this observation. Therefore, we next tested the hypothesis that MNV-1 enters cells in a caveolin 1-dependent manner. BMDMs were isolated from caveolin 1 knockout and matched wt control mice. Both wt and knockout BMDMs were infected with MNV-1 at an MOI of 2 and viral titers determined by plaque assay (Fig. 5A). No statistically significant decrease in viral titers was observed with the knockout BMDMs compared to the wt control cells over the examined time course (Fig. 5A), although knockout cells consistently produced slightly less MNV-1 than wt cells. Infections using MOIs of 0.5 and 0.05 also showed no significant decrease between the caveolin 1 knockout and wt macrophages (data not shown). These findings suggested that caveolin 1 does not play a significant role during MNV-1 infection.

To confirm these results, a caveolin 1 DN construct was also tested for its effect on MNV-1 viral gene expression. Fusion of GFP to the amino terminus of caveolin 1 prevents caveolin dimerization, and overexpression of this construct functions as a DN inhibitor (53). RAW 264.7 cells were transfected with the GFP-tagged DN construct of caveolin 1 and a control plasmid expressing only GFP and infected with MNV-1. No significant decrease in the number of VPg-expressing cells was observed

in cells transfected with the DN caveolin 1 construct compared to the GFP control-transfected cells (Fig. 5B). A trend toward a slightly decreased amount of infected cells was observed with RAW 264.7 cells, as was observed with BMDMs.

These results were also confirmed by siRNA knockdown of caveolin 1. An Accell siRNA (Dharmacon) targeted to caveolin 1 or an NT control siRNA was transfected into RAW 264.7 cells. Cells were infected with MNV-1 as described above and VPg-expressing cells enumerated. No significant decrease in the number of VPg-expressing cells was observed in the caveolin 1 siRNA-transfected cells compared to the NT control siRNA-transfected cells (Fig. 5C). Again, a slight but not statistically significant decrease in MNV-1 gene expression in caveolin 1 siRNA-transfected cells was observed, suggesting a potentially minor role for caveolin 1 during MNV-1 infection. Depletion of caveolin 1 in cells was confirmed by analyzing protein samples by immunoblotting (Fig. 5D). The relative knockdown of caveolin 1 was at $9\% \pm 4\%$ of wt levels. Together, these data demonstrate that caveolin 1 did not play a major role in MNV-1 infection of murine macrophages.

MNV-1 entry into murine macrophages is independent of phagocytosis and/or macropinocytosis. MNV-1 has a tropism for macrophages and dendritic cells (80, 84). These antigen-presenting cells are professional phagocytes (23), raising the possibility that MNV-1 entry occurs via phagocytosis. Furthermore, there is increasing evidence for the importance of macropinocytosis and/or phagocytosis as a mechanism for viral entry (45). Interestingly, although not a requirement, dynamin

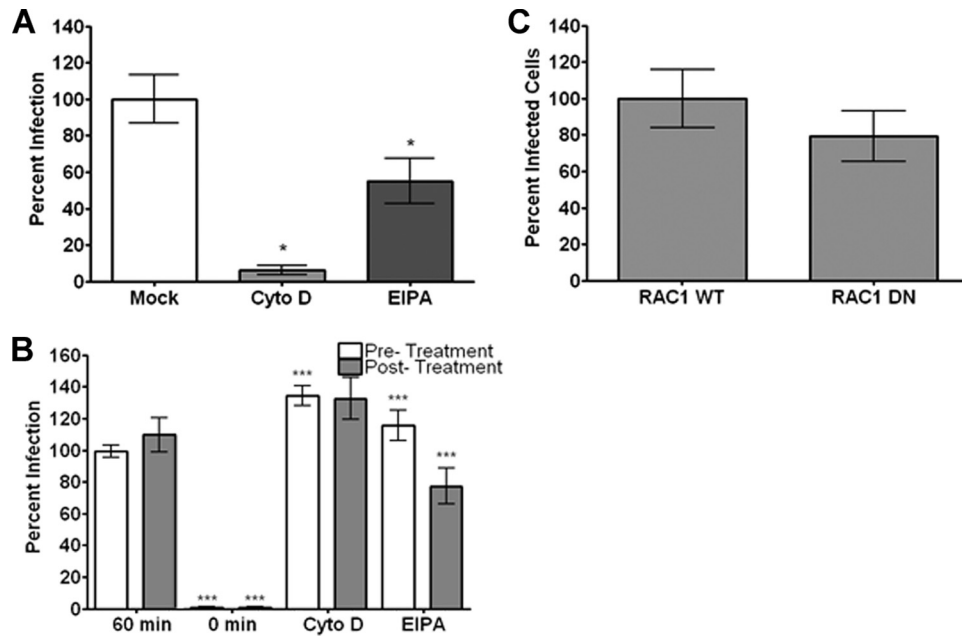


FIG. 6. MNV-1 infection is independent of phagocytosis and/or macropinocytosis. (A) RAW 264.7 cells were pretreated with 10 μ M cytochalasin D (Cyto D), 200 μ M amiloride (EIPA), or mock control before infection with *Listeria monocytogenes* strain 10403S at an MOI of 1 for 30 min at 37°C. Replication of noninternalized bacteria was inhibited with 50 μ g/ml gentamicin. After 1 h postinfection, cells were lysed and internalized bacteria plated onto LB plates. A total of 24 h after incubation at 37°C, CFU were quantitated and normalized to the value for the mock control. (B) RAW 264.7 cells were infected with NR-containing virus at an MOI of 0.001 and rocked at room temperature for 60 min. RAW 264.7 cells were either pretreated (pretreatment) or treated for 60 min pi (posttreatment) with 10 μ M cytochalasin D (cyto D), 200 μ M amiloride (EIPA), or mock control. (C) RAW 264.7 cells were transfected with a wt (RAC 1 wt) and a DN (RAC 1 DN) GFP-tagged Rac 1 and infected with MNV-1 at an MOI of 10 for 12 h. The number of VPg-expressing cells was determined by immunofluorescence and normalized to the value for the wt control. *, $P < 0.05$; ***, $P < 0.001$.

II can play a role in this process (reviewed in reference 45). Experimentally, however, it is difficult to separate the mechanisms of macropinocytosis and phagocytosis due to the similarities of these processes (reviewed in reference 45). Therefore, we are unable to distinguish an individual requirement of MNV-1 entry for either macropinocytosis or phagocytosis.

To address the importance of phagocytosis/macropinocytosis as an entry mechanism for MNV-1, we examined the effect of cytochalasin D, an inhibitor of actin polymerization, and 5-ethyl-*N*-isopropyl amiloride (EIPA), an inhibitor of macropinocytosis that blocks Na^+/H^+ exchange (82), on MNV-1 entry using the NR assay. Effective concentrations of these inhibitors in RAW 264.7 cells were determined by testing the internalization of the bacterium *L. monocytogenes* into RAW 264.7 cells in the presence of 10 μ M cytochalasin D and 200 μ M EIPA (Fig. 6A). *Listeria monocytogenes* entry into macrophages is dependent on phagocytosis, and uptake is inhibited by cytochalasin D (75). Cell viability of treated cells was unaffected at these concentrations of inhibitors (Table 1). Pretreatment of cells with cytochalasin D or EIPA did not lead to a decrease in MNV-1 infection in the NR assay (Fig. 6B). Instead, we observed a significant increase in the amount of MNV-1 entry in the presence of both inhibitors (Fig. 6B). This may be because of the upregulation of a productive route of infection by the inhibitors. Alternatively, phagocytosis/macropinocytosis may be a degradative pathway for MNV-1, and blocking this pathway leads to more viruses entering productive routes of infection. Posttreatment of cells with cytochala-

sin D had no significant effect on MNV-1 infection. Interestingly, posttreatment with EIPA showed a modest but significant decrease in the amount of MNV-1 infection (Fig. 6B), suggesting that later stages of the MNV-1 life cycle after entry are partially dependent on Na^+/H^+ exchange. Together, these data suggested that phagocytosis and/or macropinocytosis do not play a significant role in productive MNV-1 entry.

To validate this finding, we tested the requirement of Rac 1 during MNV-1 infection of RAW 264.7 cells. Rac 1 is a small GTPase required during remodeling of the cell's actin cytoskeleton to facilitate the massive membrane rearrangements necessary for phagocytosis (47). A GFP-tagged wt or DN Rac1 construct was transfected into RAW 264.7 cells and then infected with MNV-1. VPg expression was analyzed by immunofluorescence as described above (Fig. 6C). The number of VPg-expressing cells showed no significant decrease in the DN-transfected cells compared to the wt Rac 1-transfected cells (Fig. 6C). Taken together, these data demonstrated that Rac 1, which is required for phagocytosis/macropinocytosis, is not essential during MNV-1 infection. However, it is possible that phagocytic mechanisms may play a minor role during later stages in MNV-1 infection, since we observed a decrease in viral infection after EIPA posttreatment and a slight (although not statistically significant) decrease in gene expression in the presence of DN Rac1.

MNV-1 entry into murine macrophages requires cholesterol. Another form of endocytosis that requires dynamin II is cholesterol-dependent/dynamin II-dependent endocytosis,

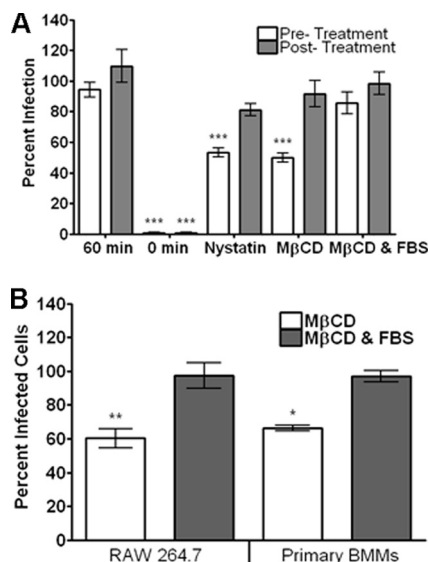


FIG. 7. MNV-1 infection is cholesterol dependent. (A) RAW 264.7 cells were infected with NR-containing virus at an MOI of 0.001 and rocked at room temperature for 60 min. RAW 264.7 cells were either pretreated (pretreatment) or treated for 60 min pi (posttreatment) with 50 μ M nystatin, 2 mM M β CD, or 2 mM M β CD with 10% fetal bovine serum (M β CD & FBS). (B) RAW 264.7 cells or BMDMs were infected with MNV-1 for 12 h after pretreatment with 2 mM M β CD or 2 mM M β CD with 10% fetal bovine serum (M β CD & FBS). The number of VPg-expressing cells was determined by immunofluorescence and normalized to the value for a no-treatment control. *, $P < 0.05$; **, $P < 0.01$; ***, $P < 0.001$.

currently an ill-defined process. Interleukin 2 receptor, the original marker protein for this endocytic pathway, was recently proposed to enter cells by a phagocytic process (22). Some viruses also enter cells in a cholesterol-dependent/dynamin II-dependent manner (51, 61, 77). To address the role of cholesterol in MNV-1 entry, we performed entry and infection assays in the presence of the cholesterol-sequestering drugs M β CD and nystatin. To determine the effect of these drugs on viral entry, RAW 264.7 cells were pretreated with 2 mM M β CD for 1 h or 50 μ M nystatin for 30 min to maintain cell viability above 80% (Table 1) and infected with NR-containing MNV-1 (Fig. 7A). We observed a significant decrease in the amount of virus entry in M β CD- or nystatin-pretreated cells but not in cells with reconstituted cholesterol levels (i.e., M β CD with FBS) (Fig. 7A). No effect on MNV-1 titers was observed when cells were treated with these drugs after infection (posttreatment) (Fig. 7A). This suggests cholesterol plays an important role during MNV-1 entry.

To verify these results for productive infection of primary macrophages, MNV-1 VPg gene expression was measured by immunofluorescence microscopy. Both RAW 264.7 cells and BMDMs were infected with MNV-1 for 12 h after pretreatment with M β CD or M β CD with FBS. Treatment with M β CD but not M β CD with FBS significantly decreased the number of infected cells in cultured and primary macrophages (Fig. 7B), confirming the importance of cholesterol during MNV-1 infection in primary cells.

High concentrations of M β CD not only inhibit cholesterol-dependent mechanisms but can also affect clathrin-mediated

endocytosis (76). Therefore, we infected RAW 264.7 cells and BMDMs with VSV after pretreatment with 2 mM M β CD and analyzed matrix protein expression by immunofluorescence. We observed no significant decrease in VSV matrix-expressing cells (data not shown). In addition, the uptake of fluorescently labeled transferrin as a marker of clathrin-mediated endocytosis was not affected by M β CD pretreatment, while internalized fluorescently labeled cholera toxin subunit B was significantly decreased (Fig. 1E, H). Hence, the levels of M β CD used herein are specific for cholesterol-dependent mechanisms. In summary, these results demonstrated an important role for cholesterol during MNV-1 entry in murine macrophages.

Flotillin-1 or GRAF 1 plays no major role during MNV-1 infection of murine macrophages. To identify further markers of MNV-1 entry, we focused on two proteins, flotillin-1 and GRAF1. Although no role during virus entry has been published to date for these proteins, flotillin-1 is a ubiquitous protein that associates with noncaveolar membrane microdomains and plays a role in some cholesterol-dependent methods of endocytosis (2). The small GTPase GRAF1 is required for another cholesterol-dependent pathway called CLIC (clathrin-independent carriers)/GEEC (GPI-enriched endocytic compartments) (37). We first tested whether MNV-1 entry requires flotillin-1. An Accell siRNA from Dharmacon targeting flotillin-1 or an NT control siRNA was transfected into RAW 264.7 cells prior to MNV-1 infection, and the number of virus-infected cells was determined by staining for VPg (Fig. 8A). No significant decrease in the number of VPg-expressing cells was observed with cells transfected with the flotillin-1 siRNA compared to those transfected with the NT control siRNA. This was despite the efficient knockdown of flotillin-1, which was confirmed by immunoblotting (Fig. 8B). The flotillin-1 protein level in flotillin-1 siRNA-transfected cells was reduced to 19% \pm 10% of the protein level in cells transfected with NT siRNA (Fig. 8B). These data suggest that flotillin-1 does not play a major role during MNV-1 infection.

The requirement for cholesterol and a direct interaction between GRAF1 and dynamin II prompted us to determine whether GRAF 1 is required for MNV-1 infection. RAW 264.7 cells were transfected with a GRAF 1 and an NT siRNA, infected with MNV-1, and analyzed for VPg expression. No significant decrease in VPg-expressing cells was observed in GRAF 1 siRNA-treated cells compared to the NT control (Fig. 8C). This was despite the successful knockdown of GRAF 1 (protein levels were reduced to 38% \pm 12% of the wt protein level) (Fig. 8D). This demonstrated that GRAF1 does not play a major role in MNV-1 uptake into macrophages, but, due to the level of GRAF 1 knockdown, a requirement of GRAF 1 in a minor route(s) of entry cannot be ruled out. Taken together, these data suggest that the major route of entry for MNV-1 is independent of flotillin-1 and GRAF1.

MNV-1 entry does not use clathrin-mediated endocytosis, caveolin-mediated endocytosis, and/or phagocytosis as a minor route of productive infection. Overall, our data demonstrate a role for both dynamin II and cholesterol during MNV-1 entry. However, no pharmacologic treatment or expression of DN construct was able to decrease MNV-1 entry or VPg expression below 20% (Fig. 3, dynasore treatment). Under most conditions, we observed a decrease of about 50% in RAW 264.7 cells and slightly less in BMDMs. This suggested

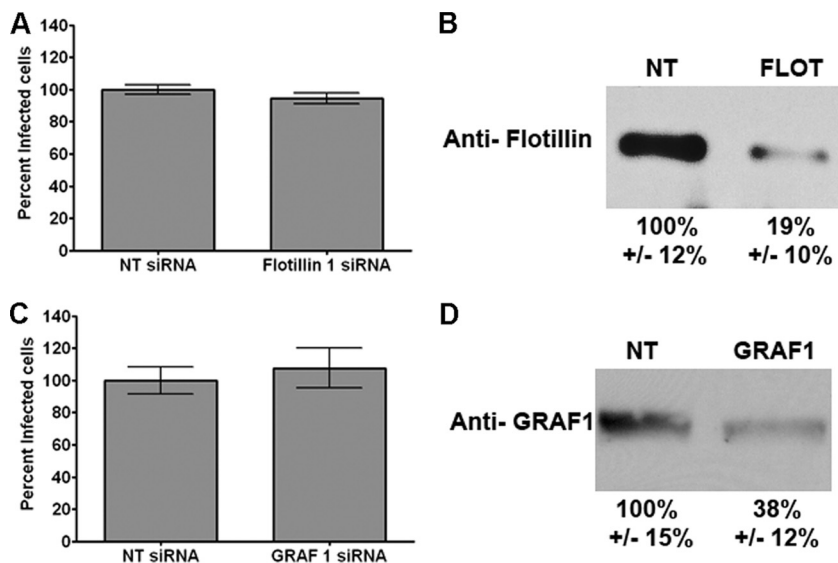


FIG. 8. The major infectious route for MNV-1 is independent of flotillin-1 and GRAF1. RAW 264.7 cells were incubated with an Accell siRNA against flotillin-1 (A), GRAF1 (C), or a nontargeting (NT) construct (A and C) (Dharmacon) for 72 h. Cells were then infected with MNV-1 at an MOI of 10, and VPg expression was determined by immunofluorescence 12 h after infection. To verify flotillin-1 (FLOT) (B) or GRAF1 (D) protein knockdown, protein samples of cells transfected with the respective siRNA construct were analyzed by immunoblotting for flotillin-1 or GRAF1 and quantitated as described in the text.

that either these inhibitors or DN constructs are unable to fully inhibit these processes or that the virus can productively enter the cell by more than one pathway. Virus entering cells via multiple routes has previously been reported, e.g., influenza A virus (32) and SV40 (14). To test the hypothesis that MNV-1 enters cells by more than one productive pathway, we tested combinations of inhibitors in the NR assay (Fig. 9). We pretreated RAW 264.7 cells with combinations of MβCD and other inhibitors (nystatin, chlorpromazine, dynasore, cytochalasin D, and EIPA), infected the cells with NR-containing MNV-1, and performed the NR assay. No significant decrease in MNV-1 entry was observed in the combination treatments compared to the MβCD-only treatment. Inhibition of dynamin II by addition of dynasore and MβCD did not significantly

decrease viral entry further compared to addition of MβCD alone, suggesting that clathrin-mediated and caveolin-mediated endocytosis did not play a role in MNV-1 infection. Similar results were obtained with EIPA or cytochalasin D and MβCD, suggesting that phagocytosis/macropinocytosis did not play a role during MNV-1 entry. Interestingly, a significant increase in viral entry was observed in MβCD- and chlorpromazine-treated cells (Fig. 9), despite a decrease of cell viability to approximately 60% of untreated controls (Table 1). Taken together, these data suggest that clathrin-mediated endocytosis, caveolin-mediated endocytosis, and phagocytosis/macropinocytosis did not play minor roles during MNV-1 infection in RAW 264.7 cells.

DISCUSSION

Many viruses require the cellular mechanism of endocytosis to productively infect their host. The mechanism of entry during the productive route of infection for noroviruses has not been addressed previously due to the lack of an efficient cell culture system. However, it has been suggested that the early steps of infection, including entry, are the determinants of cell tropism for this understudied group of viruses (24). Herein, we used a combination of pharmacologic inhibitor studies, dominant-negative mutants, and siRNA knockdowns, with a newly adapted neutral red assay to study the infectious route of entry of MNV-1. These data demonstrate that MNV-1 uptake occurs rapidly (within 1 h) and that the productive route of entry of MNV-1 into murine macrophages requires both host cholesterol and dynamin II. We also showed that the major route of MNV-1 infection of murine macrophages neither is clathrin, caveolin, flotillin-1, or GRAF1 dependent nor involves phagocytosis and/or macropinocytosis. During submission of this article, Gerondopoulos et al. published a report (20) demonstrat-

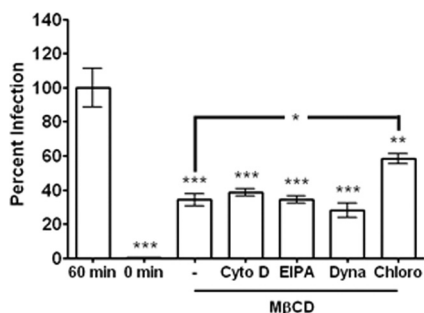


FIG. 9. Clathrin- and caveolin-dependent endocytosis or phagocytosis/macropinocytosis are not a minor route of entry for MNV-1. RAW 264.7 cells were pretreated with 2 mM MβCD alone (-), 2 mM MβCD and 10 μM cytochalasin D (cyto D), 2 mM MβCD and 200 μM amiloride (EIPA), 2 mM MβCD and 80 μM dynasore (Dyna), or 2 mM MβCD and 40 μM chlorpromazine (Chloro). RAW 264.7 cells were infected with NR-containing virus at an MOI of 0.001 and rocked at room temperature for 60 min before performing the NR assay and determining viral titers. *, *P* < 0.05; **, *P* < 0.01; ***, *P* < 0.001.

ing that MNV-1 entry into RAW 264.7 cells is mediated by dynamin and cholesterol but independent of clathrin, caveolin, flotillin-1, and macropinocytosis, confirming our findings with those cells.

While little is known about calicivirus entry, FCV enters cells via clathrin-mediated endocytosis (65). Our data clearly demonstrated that clathrin does not play a role during the productive route of infection of murine macrophages by MNV-1 (Fig. 4). This further highlights the differences during virus entry between these two viruses, as FCV (65), in contrast to MNV-1 (54), enters cells in a pH-dependent manner. Whether these entry differences reflect differences in the pathogenesis of a respiratory (FCV) versus an enteric (MNV-1) virus and/or differences in the examined cell types (epithelial cells versus macrophages) remains unknown. In addition, a requirement for host cholesterol during HuNoV replication is known. Inhibitors of cholesterol synthesis significantly reduced HuNoV replication in a HuNoV replicon system (9). Although the direct role of cholesterol during MNV-1 replication was not addressed here, the common requirement for host cholesterol during MNV-1 and HuNoV infection suggests a conservation of cellular constituents during norovirus infection.

The mechanism of cholesterol- and dynamin II-dependent endocytosis is not well defined. Few viruses are reported to enter cells in this manner. Feline infectious peritonitis virus (FIPV) infection of monocytes, a macrophage precursor, is sensitive to the cholesterol-sequestering drug nystatin (but not M β CD) and dynasore (77). Group B coxsackievirus 3 (CVB3) infection of HeLa cells is inhibited by the dynamin II DN construct, K44A, dynasore, M β CD, and filipin treatment (51). Furthermore, rotavirus entry into MA104 cells is inhibited by the K44A DN mutant of dynamin II and by depletion of cholesterol with M β CD but not the other cholesterol-sequestering drugs nystatin and filipin (61). Similar to our results with MNV-1 (Fig. 3 and 7), inhibition of dynamin II or cholesterol depletion only partially reduced entry of FIPV, CVB3, and rotavirus. Whether this reflects an inherent ability of cells to compensate for blocked endocytic pathways and/or an ability of viruses to use more than one entry pathway remains unknown.

We investigated the role of alternative or minor routes of MNV-1 entry by treatments with combinations of inhibitors in the NR assay. Although no combination of inhibitors showed a significant decrease in the amount of MNV-1 entry over M β CD treatment alone, we observed a significant increase in the amount of viral entry occurring in the presence of both M β CD and chlorpromazine. This increase was observed despite a decrease in the cell viability to approximately 60% of the untreated control. Although the biological significance of this finding is unclear, this result suggested that MNV-1 can enter RAW 264.7 cells by a clathrin- and cholesterol-independent pathway that is upregulated by treatment with chlorpromazine and M β CD.

In this report, we identified a requirement for cholesterol and dynamin II during MNV-1 entry. However, specific cellular targets of the host endocytic machinery interacting with MNV-1 during this stage in the viral life cycle remain elusive. Further definition of the mechanism of MNV-1 entry will not only better describe a poorly defined endocytic pathway but

may also lead to the identification of cellular targets with antinoroviral potential.

ACKNOWLEDGMENTS

This work was funded by start-up funds from the University of Michigan and NIH/NIAID R01 AI080611 to C.E.W. J.W.P. was funded by the University of Michigan Human Genetics training grant (grant NIH T32 GM 07544) and the Molecular Mechanisms of Microbial Pathogenesis training grant (NIH T32 AI 007528).

We thank Ian Clark (University of Southampton, United Kingdom; anti-VPg), Richard Lundmark (Umeå University, Sweden; anti-GRAF1), and John Connor (Boston University; anti-VSV matrix) for their generous gifts of antibodies. We also thank Mark McNiven (Mayo Institute, Rochester, MN; dynamin II constructs), Alexandre Benmerah (INSERM, Paris, France; EPS15 constructs), Joel Swanson (University of Michigan, Ann Arbor, MI; GFP and RAC 1 constructs), and Billy Tsai (University of Michigan, Ann Arbor, MI; caveolin 1 construct) for plasmids and Mary O'Riordan for *L. monocytogenes*. We are indebted to the Center for Statistical Consultation and Research at the University of Michigan for advice on statistical analysis and to Kathy Spindler (University of Michigan, Ann Arbor, MI) for critical reading of the manuscript.

REFERENCES

- Anderson, H. A., Y. Chen, and L. C. Norkin. 1996. Bound simian virus 40 translocates to caveolin-enriched membrane domains, and its entry is inhibited by drugs that selectively disrupt caveolae. *Mol. Biol. Cell* **7**:1825–1834.
- Babuke, T., and R. Tikkanen. 2007. Dissecting the molecular function of reggie/flotillin proteins. *Eur. J. Cell Biol.* **86**:525–532.
- Belleudi, F., V. Visco, M. Ceridono, L. Leone, R. Muraro, L. Frati, and M. R. Torrisi. 2003. Ligand-induced clathrin-mediated endocytosis of the keratinocyte growth factor receptor occurs independently of either phosphorylation or recruitment of eps15. *FEBS Lett.* **553**:262–270.
- Benmerah, A., M. Bayrou, N. Cerf-Bensussan, and A. Dautry-Varsat. 1999. Inhibition of clathrin-coated pit assembly by an Eps15 mutant. *J. Cell Sci.* **112**:1303–1311.
- Blanton, L. H., S. M. Adams, R. S. Beard, G. Wei, S. N. Bulens, M. A. Widdowson, R. I. Glass, and S. S. Monroe. 2006. Molecular and epidemiologic trends of caliciviruses associated with outbreaks of acute gastroenteritis in the United States, 2000–2004. *J. Infect. Dis.* **193**:413–421.
- Borrow, P., and M. B. Oldstone. 1994. Mechanism of lymphocytic choriomeningitis virus entry into cells. *Virology* **198**:1–9.
- Brandenburg, B., L. Y. Lee, M. Lakadamyali, M. J. Rust, X. Zhuang, and J. M. Hogle. 2007. Imaging poliovirus entry in live cells. *PLoS Biol.* **5**:e183.
- Cao, H., H. M. Thompson, E. W. Krueger, and M. A. McNiven. 2000. Disruption of Golgi structure and function in mammalian cells expressing a mutant dynamin. *J. Cell Sci.* **113**:1993–2002.
- CDC. 2007. Norovirus activity—United States, 2006–2007. *MMWR Morb. Mortal. Wkly. Rep.* **56**:842–846.
- Chang, K. O. 2009. Role of cholesterol pathways in norovirus replication. *J. Virol.* **83**:8587–8595.
- Chaudhry, Y., M. A. Skinner, and I. G. Goodfellow. 2007. Recovery of genetically defined murine norovirus in tissue culture by using a fowlpox virus expressing T7 RNA polymerase. *J. Gen. Virol.* **88**:2091–2100.
- Clement, C., V. Tiwari, P. M. Scanlan, T. Valyi-Nagy, B. Y. Yue, and D. Shukla. 2006. A novel role for phagocytosis-like uptake in herpes simplex virus entry. *J. Cell Biol.* **174**:1009–1021.
- Conner, S. D., and S. L. Schmid. 2003. Regulated portals of entry into the cell. *Nature* **422**:37–44.
- Coyne, C. B., L. Shen, J. R. Turner, and J. M. Bergelson. 2007. Coxsackievirus entry across epithelial tight junctions requires occludin and the small GTPases Rab34 and Rab5. *Cell Host Microbe* **2**:181–192.
- Damm, E. M., L. Pelkmans, J. Kartenbeck, A. Mezzacasa, T. Kurzchalia, and A. Helenius. 2005. Clathrin- and caveolin-1-independent endocytosis: entry of simian virus 40 into cells devoid of caveolae. *J. Cell Biol.* **168**:477–488.
- Dautry-Varsat, A. 1986. Receptor-mediated endocytosis: the intracellular journey of transferrin and its receptor. *Biochimie* **68**:375–381.
- De Camilli, P., K. Takei, and P. S. McPherson. 1995. The function of dynamin in endocytosis. *Curr. Opin. Neurobiol.* **5**:559–565.
- Doherty, G. J., and H. T. McMahon. 2009. Mechanisms of endocytosis. *Annu. Rev. Biochem.* **78**:857–902.
- Estes, M. K., B. V. Prasad, and R. L. Atmar. 2006. Noroviruses everywhere: has something changed? *Curr. Opin. Infect. Dis.* **19**:467–474.
- Fankhauser, R. L., S. S. Monroe, J. S. Noel, C. D. Humphrey, J. S. Breese, U. D. Parashar, T. Ando, and R. I. Glass. 2002. Epidemiologic and molecular trends of “Norwalk-like viruses” associated with outbreaks of gastroenteritis in the United States. *J. Infect. Dis.* **186**:1–7.

20. Gerondopoulos, A., T. Jackson, P. Monaghan, N. Doyle, and L. O. Roberts. 2010. Murine norovirus-1 cell entry is mediated through a non-clathrin, non-caveolae, dynamin and cholesterol dependent pathway. *J. Gen. Virol.* [Epub ahead of print] doi:10.1099/vir.0.016717-0.
21. Ghigo, E., J. Kartenbeck, P. Lien, L. Pelkmans, C. Capo, J. L. Mege, and D. Raouf. 2008. Ameobal pathogen mimivirus infects macrophages through phagocytosis. *PLoS Pathog.* 4:e1000087.
22. Grassart, A., A. Dujancourt, P. B. Lazarow, A. Dautry-Varsat, and N. Sauvonnnet. 2008. Clathrin-independent endocytosis used by the IL-2 receptor is regulated by Rac1, Pak1 and Pak2. *EMBO Rep.* 9:356–362.
23. Groves, E., A. E. Dart, V. Covarelli, and E. Caron. 2008. Molecular mechanisms of phagocytic uptake in mammalian cells. *Cell. Mol. Life Sci.* 65: 1957–1976.
24. Guix, S., M. Asanaka, K. Katayama, S. E. Crawford, F. H. Neill, R. L. Atmar, and M. K. Estes. 2007. Norwalk virus RNA is infectious in mammalian cells. *J. Virol.* 81:12238–12248.
25. Henley, J. R., E. W. Krueger, B. J. Oswald, and M. A. McNiven. 1998. Dynamin-mediated internalization of caveolae. *J. Cell Biol.* 141:85–99.
26. Heuser, J. E., and R. G. Anderson. 1989. Hypertonic media inhibit receptor-mediated endocytosis by blocking clathrin-coated pit formation. *J. Cell Biol.* 108:389–400.
- 26a. Hoppe, A. D., and J. A. Swanson. 2004. Cdc42, Rac1, and Rac2 display distinct patterns of activation during phagocytosis. *Mol. Biol. Cell* 15:3509–3519.
27. Karst, S. M., C. E. Wobus, M. Lay, J. Davidson, and H. W. Virgin IV. 2003. STAT1-dependent innate immunity to a Norwalk-like virus. *Science* 299: 1575–1578.
28. Kartenbeck, J., H. Stukenbrok, and A. Helenius. 1989. Endocytosis of simian virus 40 into the endoplasmic reticulum. *J. Cell Biol.* 109:2721–2729.
29. Katpally, U., N. R. Voss, T. Cavazza, S. Taube, J. R. Rubin, V. L. Young, J. Stuckey, V. K. Ward, H. W. Virgin IV, C. E. Wobus, and T. J. Smith. 24 March 2010. High-resolution cryo-electron microscopy structures of MNV-1 and RHDV reveals marked flexibility in the receptor binding domains. *J. Virol.* doi:10.1128/JVI.00314-10.
30. Katpally, U., C. E. Wobus, K. Dryden, H. W. Virgin IV, and T. J. Smith. 2008. Structure of antibody-neutralized murine norovirus and unexpected differences from viruslike particles. *J. Virol.* 82:2079–2088.
31. Koopmans, M., J. Vinje, M. de Wit, I. Leenen, W. van der Poel, and Y. van Duynhoven. 2000. Molecular epidemiology of human enteric calciviruses in The Netherlands. *J. Infect. Dis.* 181(Suppl. 2):S262–S269.
32. Lakadamyali, M., M. J. Rust, H. P. Babcock, and X. Zhuang. 2003. Visualizing infection of individual influenza viruses. *Proc. Natl. Acad. Sci. U. S. A.* 100:9280–9285.
33. Le Pendu, J. 2004. Histo-blood group antigen and human milk oligosaccharides: genetic polymorphism and risk of infectious diseases. *Adv. Exp. Med. Biol.* 554:135–143.
34. Le Pendu, J., N. Ruvoen-Clouet, E. Kindberg, and L. Svensson. 2006. Mendelian resistance to human norovirus infections. *Semin. Immunol.* 18:375–386.
35. Lindesmith, L., C. Moe, S. Marionneau, N. Ruvoen, X. Jiang, L. Lindblad, P. Stewart, J. LePend, and R. Baric. 2003. Human susceptibility and resistance to Norwalk virus infection. *Nat. Med.* 9:548–553.
36. Liu, N. Q., A. S. Lossinsky, W. Popik, X. Li, C. Gajuluva, B. Kriederman, J. Roberts, T. Pushkarsky, M. Bukrinsky, M. Witte, M. Weinand, and M. Fiala. 2002. Human immunodeficiency virus type 1 enters brain microvascular endothelia by macropinocytosis dependent on lipid rafts and the mitogen-activated protein kinase signaling pathway. *J. Virol.* 76:6689–6700.
37. Lundmark, R., G. J. Doherty, M. T. Howes, K. Cortese, Y. Vallis, R. G. Parton, and H. T. McMahon. 2008. The GTPase-activating protein GRAF1 regulates the CLIC/GEEC endocytic pathway. *Curr. Biol.* 18:1802–1808.
38. Lyles, D. S., L. Puddington, and B. J. McCreedy, Jr. 1988. Vesicular stomatitis virus M protein in the nuclei of infected cells. *J. Virol.* 62:4387–4392.
39. Macia, E., M. Ehrlich, R. Massol, E. Boucrot, C. Brunner, and T. Kirchhausen. 2006. Dynasore, a cell-permeable inhibitor of dynamin. *Dev. Cell* 10:839–850.
40. Maréchal, V., M. C. Prevost, C. Petit, E. Perret, J. M. Heard, and O. Schwartz. 2001. Human immunodeficiency virus type 1 entry into macrophages mediated by macropinocytosis. *J. Virol.* 75:11166–11177.
41. Marsh, M., and A. Helenius. 2006. Virus entry: open sesame. *Cell* 124:729–740.
42. Matilainen, H., J. Rinne, L. Gilbert, V. Marjomaki, H. Reunanen, and C. Oker-Blom. 2005. Baculovirus entry into human hepatoma cells. *J. Virol.* 79:15452–15459.
43. Mead, P. S., L. Slutsker, V. Dietz, L. F. McCaig, J. S. Bresee, C. Shapiro, P. M. Griffin, and R. V. Tauxe. 1999. Food-related illness and death in the United States. *Emerg. Infect. Dis.* 5:607–625.
44. Meier, O., K. Boucke, S. V. Hammer, S. Keller, R. P. Stidwill, S. Hemmi, and U. F. Greber. 2002. Adenovirus triggers macropinocytosis and endosomal leakage together with its clathrin-mediated uptake. *J. Cell Biol.* 158:1119–1131.
45. Mercer, J., and A. Helenius. 2009. Virus entry by macropinocytosis. *Nat. Cell Biol.* 11:510–520.
46. Moreno-Espinosa, S., T. Farkas, and X. Jiang. 2004. Human calciviruses and pediatric gastroenteritis. *Semin. Pediatr. Infect. Dis.* 15:237–245.
47. Niedergang, F., and P. Chavrier. 2005. Regulation of phagocytosis by Rho GTPases. *Curr. Top. Microbiol. Immunol.* 291:43–60.
48. Norkin, L. C., H. A. Anderson, S. A. Wolfrom, and A. Oppenheim. 2002. Caveolar endocytosis of simian virus 40 is followed by brefeldin A-sensitive transport to the endoplasmic reticulum, where the virus disassembles. *J. Virol.* 76:5156–5166.
49. Obar, R. A., C. A. Collins, J. A. Hammarback, H. S. Shpetner, and R. B. Vallee. 1990. Molecular cloning of the microtubule-associated mechanochemical enzyme dynamin reveals homology with a new family of GTP-binding proteins. *Nature* 347:256–261.
50. Oh, P., D. P. McIntosh, and J. E. Schnitzer. 1998. Dynamin at the neck of caveolae mediates their budding to form transport vesicles by GTP-driven fission from the plasma membrane of endothelium. *J. Cell Biol.* 141:101–114.
51. Patel, K. P., C. B. Coyne, and J. M. Bergelson. 2009. Dynamin- and lipid raft-dependent entry of decay-accelerating factor (DAF)-binding and non-DAF-binding coxsackieviruses into nonpolarized cells. *J. Virol.* 83:11064–11077.
52. Pelkmans, L., T. Burli, M. Zerial, and A. Helenius. 2004. Caveolin-stabilized membrane domains as multifunctional transport and sorting devices in endocytic membrane traffic. *Cell* 118:767–780.
53. Pelkmans, L., J. Kartenbeck, and A. Helenius. 2001. Caveolar endocytosis of simian virus 40 reveals a new two-step vesicular-transport pathway to the ER. *Nat. Cell Biol.* 3:473–483.
54. Perry, J. W., S. Taube, and C. E. Wobus. 2009. Murine norovirus-1 entry into permissive macrophages and dendritic cells is pH-independent. *Virus Res.* 143:125–129.
55. Pietiäinen, V., V. Marjomaki, P. Upla, L. Pelkmans, A. Helenius, and T. Hyypia. 2004. Echovirus 1 endocytosis into caveosomes requires lipid rafts, dynamin II, and signaling events. *Mol. Biol. Cell* 15:4911–4925.
56. Pietiäinen, V. M., V. Marjomaki, J. Heino, and T. Hyypia. 2005. Viral entry, lipid rafts and caveosomes. *Ann. Med.* 37:394–403.
57. Quirin, K., B. Eschli, I. Scheu, L. Poort, J. Kartenbeck, and A. Helenius. 2008. Lymphocytic choriomeningitis virus uses a novel endocytic pathway for infectious entry via late endosomes. *Virology* 378:21–33.
58. Rojek, J. M., M. Perez, and S. Kunz. 2008. Cellular entry of lymphocytic choriomeningitis virus. *J. Virol.* 82:1505–1517.
59. Rust, M. J., M. Lakadamyali, F. Zhang, and X. Zhuang. 2004. Assembly of endocytic machinery around individual influenza viruses during viral entry. *Nat. Struct. Mol. Biol.* 11:567–573.
60. Rydell, G. E., J. Nilsson, J. Rodriguez-Diaz, N. Ruvoen-Clouet, L. Svensson, J. Le Pendu, and G. Larson. 2009. Human noroviruses recognize sialyl Lewis x neoglycoprotein. *Glycobiology* 19:309–320.
61. Sánchez-San Martín, C., T. Lopez, C. F. Arias, and S. Lopez. 2004. Characterization of rotavirus cell entry. *J. Virol.* 78:2310–2318.
62. Reference deleted.
63. Sieczkarski, S. B., and G. R. Whittaker. 2002. Dissecting virus entry via endocytosis. *J. Gen. Virol.* 83:1535–1545.
64. Spoden, G., K. Freitag, M. Husmann, K. Boller, M. Sapp, C. Lambert, and L. Florin. 2008. Clathrin- and caveolin-independent entry of human papillomavirus type 16— involvement of tetraspanin-enriched microdomains (TEMs). *PLoS One* 3:e3313.
65. Stuart, A. D., and T. D. Brown. 2006. Entry of feline calicivirus is dependent on clathrin-mediated endocytosis and acidification in endosomes. *J. Virol.* 80:7500–7509.
66. Sun, X., V. K. Yau, B. J. Briggs, and G. R. Whittaker. 2005. Role of clathrin-mediated endocytosis during vesicular stomatitis virus entry into host cells. *Virology* 338:53–60.
67. Taguchi, N., N. Ishihara, A. Jofuku, T. Oka, and K. Mihara. 2007. Mitotic phosphorylation of dynamin-related GTPase Drp1 participates in mitochondrial fission. *J. Biol. Chem.* 282:11521–11529.
68. Takei, K., P. S. McPherson, S. L. Schmid, and P. De Camilli. 1995. Tubular membrane invaginations coated by dynamin rings are induced by GTP-gamma S in nerve terminals. *Nature* 374:186–190.
69. Tamura, M., K. Natori, M. Kobayashi, T. Miyamura, and N. Takeda. 2004. Genogroup II noroviruses efficiently bind to heparan sulfate proteoglycan associated with the cellular membrane. *J. Virol.* 78:3817–3826.
70. Tan, M., and X. Jiang. 2007. Norovirus-host interaction: implications for disease control and prevention. *Expert Rev. Mol. Med.* 9:1–22.
71. Tan, M., and X. Jiang. 2005. Norovirus and its histo-blood group antigen receptors: an answer to a historical puzzle. *Trends Microbiol.* 13:285–293.
72. Taube, S., J. W. Perry, K. Yetming, S. P. Patel, H. Auble, L. Shu, H. F. Nawar, C. H. Lee, T. D. Connell, J. A. Shayman, and C. E. Wobus. 2009. Ganglioside-linked terminal sialic acid moieties on murine macrophages function as attachment receptors for murine noroviruses. *J. Virol.* 83:4092–4101.
73. Taube, S., J. R. Rubin, U. Katpally, T. J. Smith, A. Kendall, J. A. Stuckey, and C. E. Wobus. 24 March 2010. High resolution x-ray structure and functional analysis of the murine norovirus (MNV)-1 capsid protein protruding (P) domain. *J. Virol.* [Epub ahead of print]. doi:10.1128/JVI.00316-10.

74. **Thackray, L. B., C. E. Wobus, K. A. Chachu, B. Liu, E. R. Alegre, K. S. Henderson, S. T. Kelley, and H. W. Virgin IV.** 2007. Murine noroviruses comprising a single genogroup exhibit biological diversity despite limited sequence divergence. *J. Virol.* **81**:10460–10473.
75. **Tilney, L. G., and D. A. Portnoy.** 1989. Actin filaments and the growth, movement, and spread of the intracellular bacterial parasite, *Listeria monocytogenes*. *J. Cell Biol.* **109**:1597–1608.
76. **Ürs, N. M., K. T. Jones, P. D. Salo, J. E. Severin, J. Trejo, and H. Radhakrishna.** 2005. A requirement for membrane cholesterol in the beta-arrestin- and clathrin-dependent endocytosis of LPA1 lysophosphatidic acid receptors. *J. Cell Sci.* **118**:5291–5304.
77. **Van Hamme, E., H. L. Dewerchin, E. Cornelissen, B. Verhasselt, and H. J. Nauwynck.** 2008. Clathrin- and caveolae-independent entry of feline infectious peritonitis virus in monocytes depends on dynamin. *J. Gen. Virol.* **89**:2147–2156.
78. **Vidricaire, G., and M. J. Tremblay.** 2007. A clathrin, caveolae, and dynamin-independent endocytic pathway requiring free membrane cholesterol drives HIV-1 internalization and infection in polarized trophoblastic cells. *J. Mol. Biol.* **368**:1267–1283.
79. **Wang, L. H., K. G. Rothberg, and R. G. Anderson.** 1993. Mis-assembly of clathrin lattices on endosomes reveals a regulatory switch for coated pit formation. *J. Cell Biol.* **123**:1107–1117.
80. **Ward, J. M., C. E. Wobus, L. B. Thackray, C. R. Erexson, L. J. Faucette, G. Belliot, E. L. Barron, S. V. Sosnovtsev, and K. Y. Green.** 2006. Pathology of immunodeficient mice with naturally occurring murine norovirus infection. *Toxicol. Pathol.* **34**:708–715.
81. **Ward, V. K., C. J. McCormick, I. N. Clarke, O. Salim, C. E. Wobus, L. B. Thackray, H. W. Virgin IV, and P. R. Lambden.** 2007. Recovery of infectious murine norovirus using pol II-driven expression of full-length cDNA. *Proc. Natl. Acad. Sci. U. S. A.* **104**:11050–11055.
82. **West, M. A., M. S. Bretscher, and C. Watts.** 1989. Distinct endocytotic pathways in epidermal growth factor-stimulated human carcinoma A431 cells. *J. Cell Biol.* **109**:2731–2739.
83. **Widdowson, M. A., S. S. Monroe, and R. I. Glass.** 2005. Are noroviruses emerging? *Emerg. Infect. Dis.* **11**:735–737.
84. **Wobus, C. E., S. M. Karst, L. B. Thackray, K. O. Chang, S. V. Sosnovtsev, G. Belliot, A. Krug, J. M. Mackenzie, K. Y. Green, and H. W. Virgin.** 2004. Replication of norovirus in cell culture reveals a tropism for dendritic cells and macrophages. *PLoS Biol.* **2**:e432.